

Supporting Information

Catalytic templating approaches for three-dimensional hollow carbon/graphene oxide nano-architectures

Gun-hee Moon,^{†‡} Yongsoon Shin,^{*,†} Daiwon Choi,[†] Bruce W. Arey,[†] Gregory J. Exarhos,[†] Chongmin Wang,[†] Wonyong Choi,^{*,‡} and Jun Liu^{*,†}

[†]*Chemicals & Materials Sciences Division, Pacific Northwest National Laboratory (PNNL), 902 Battelle Boulevard, Richland, Washington, 99354, USA*

[‡]*Department of Chemical Engineering, Pohang University of Science and Technology (POSTECH), Pohang, 790-784, Republic of Korea*

Experimental Details

Synthesis of GO: Graphite oxide was prepared by the oxidation of graphite (Natural graphite, SP-1 Bay carbon) using the modified Hummer method.¹ Graphite oxide (0.125 g) was added in purified water (50 mL) and then was exfoliated into monolayer GO by sonication in an ultrasonic bath (135W, 8893, Cole-Parmer Ins.) for 2 h.

Synthesis of ACS template: Aqueous ammonia hydroxide (2.5 mL, 30 wt %, Fisher Chemicals) was dissolved in the solution containing purified water (10 mL) and ethanol (74 mL, Absolute ACS/USP grade, Pharmco-AAPER) then TEOS (6 mL, Aldrich) was added under vigorous stirring.² After the reaction for 24 h, the solution containing TEOS (5 mL) and C₁₈TMS (2 mL, 95 %, Gelest Inc.) was added into the reactor and then was kept for 4 h to make mesoporous shells. The sample collected by centrifuge at 11,000 rpm for 30 min was dried for 12 h in air then was grinded to make fine powder. After the calcination at 550 °C in air for 6h, 1 g of silica powder was added into the solution (0.2 g of AlCl₃•6H₂O (Aldrich) + 1 mL of purified water) and then was kept for 3 h under mild stirring to incorporate aluminum. The sample was dried at 85 °C for 4 h, and was grinded again. Finally, ACS template was obtained by calcination at 550 °C in air for 6h.

Hollow carbon/graphene oxide composites and thermal reduction: For self-assembly of ACS with GO, 0.5 g of the ACS template was added into the mixture (GO suspension + 1 mL of EtOH), sonicated, and then vacuum filtered. To prepare HCS/r-GO5, HCS/r-GO15, and HCS/r-GO25 composites with different amount of r-GO, GO-suspended solution (2.5 mg mL⁻¹) of 5, 15, and 25 mL was employed, respectively, and the total volume of the mixture was fixed to 50 mL by adding water before sonication. The ACS/GO samples were dried at 85°C overnight and were ground into a fine powder. The mixture of ACS/GO powder (0.5 g) and phenol (0.187 g, ≥99%, Aldrich) was kept at 100°C for 12 h under vacuum. Then, paraformaldehyde (0.119 g, Aldrich) was added and remained at 130°C for 24 h under vacuum for polymerization. The pure ACS template also was used for preparing the HCS. All

samples were calcined at 900°C for more than 6 h under Ar gas flow (with 2.7% H₂), and the heating rate was 3°C min⁻¹. After calcination, the samples were added into the solution (30 mL of water + 30 mL of hydrofluoric acid (48 wt%, Aldrich) + 30 mL of EtOH) and were kept for 3 h under vigorous stirring. The HCS/r-GO products were filtered and washed by water until neutralization then dried at 85°C for 3 h. For the KOH activation, 100 mg of the HCS/r-GO5 sample was added to 400-mg KOH in water (5 mL). The mixture was kept at 60°C for 4 h and heated to 100°C to evaporate the extra water. The powder was treated at 800°C for 1 h in 2.7% H₂/Ar gas. The treated powder was washed with 1 M HCl and with extra deionized (DI) water followed by air drying at 85°C overnight under vacuum.

Characterization: The morphologies were studied via field emission scanning electron microscopy (FE-SEM) JEOL-JSEM 633F and transmission electron microscopy (TEM) JEOL JEM 2010. The nitrogen adsorption and desorption isotherms were measured using AUTOSORB-6 (Quantachrome Inc.). Before measurement, all samples were degased at 200 °C for overnight. The electrical conductivity of free-standing films of GO and r-GO was collected by Hall effect measurement system (HMS-5000, Ecopia) at room temperature. X-ray diffraction (XRD) data were obtained by a Philips X'ert MPD X-ray diffractometer. FT-IR spectra were recorded over 400-4000 cm⁻¹ with a resolution of 4 cm⁻¹ using a Nexus 670 FT-IR spectrometer (Thermal Nicolet) based on KBr pellet method. G and D band of carbon were measured by Raman spectroscopy with peak uncertainty estimated ± 1.0 cm⁻¹, which were collected in the backscattering configuration using a Spex Model 1877 spectrometer (Edison, NJ). A liquid N₂ cooled charge-coupled detector (LN/CCD) and the 488 nm line of a Coherent Innova 307 Argon ion laser (Santa Clara, CA) for excitation were utilized.. Baseline correction was achieved using Winspec software (Princeton Instruments)

Electrochemical performance: The electrochemical test was measured by CHI 660C potentiostat with three-electrode system under an aqueous 2 M H₂SO₄ electrolyte. A Pt wire

and a Ag/AgCl electrode were used as the counter and reference electrodes, respectively.

Before the sample loading on the glassy carbon electrode (CHI103, 3mm) as a working electrode, polishing by alumina slurry, sonication for 3 min, and drying under N₂ atmosphere for overnight were sequentially followed. 4 mg of the sample was added into 2 mL of EtOH, and then was sonicated in an ultrasonic bath for 5 min. The solution of 10 µL was loaded on the glassy carbon electrode by drop casting. After evaporation of ethanol, Nafion of 10 µL was loaded again to fix the sample on the electrode. All electrodes were immersed in 2M H₂SO₄ aqueous solution for overnight to increase the wettability, and cycling was repeated until stabilization of CV curves before measurement. Two electrode processing was performed in an air-tight supercapacitor cells.³ In a two –electrode system for supercapacitance measurement the composite powder smaples are mixed with PTFE (polytetrafluoroethylene, 60% in H₂O) and coated on the Al-foil current collector. The active material used consisted of 95% of sample and 5% of the binder. Before the assembling of the working electrodes, composite materials were heated at $T = 150\text{ }^{\circ}\text{C}$ during 24 h under reduced pressure ($p < 10^{-3}\text{ atm}$). All the electrochemical experiments were made inside the glove box under very clean and dry conditions (O₂ and H₂O concentration lower than 1 ppm). Between working electrodes the 25 µm thick Celgard 2400 separator sheet was used. The amount of the composite materials was kept constant for each electrode. The cell is then immersed in the electrolyte and is placed in an argon-filled sealed box. Galvanostatic cycling of supercapacitor cells was performed using a Solatron 2225B potentiostat at variable current densities of between 0 and 2 V.

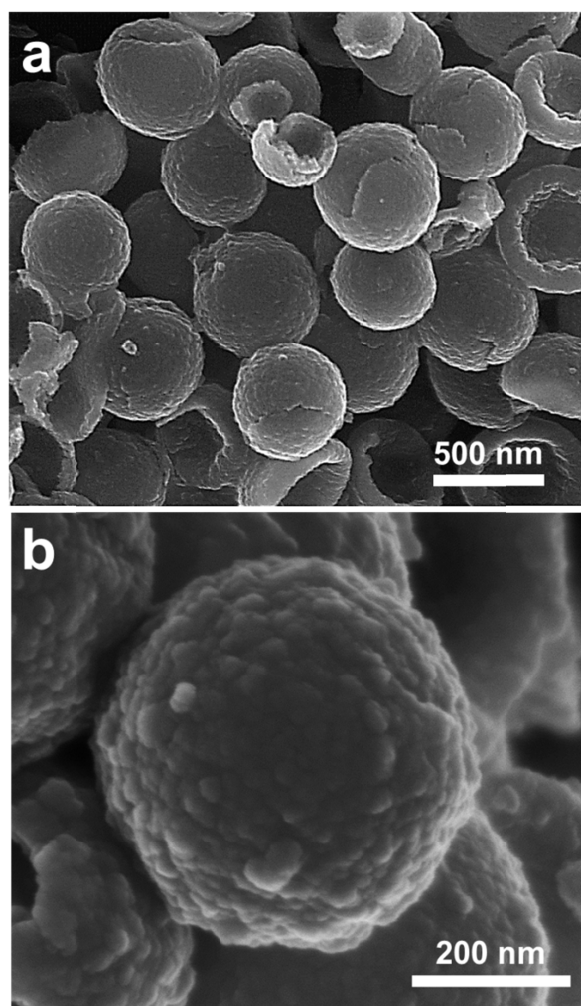


Figure S1. SEM images of hollow carbon spheres with small carbon granules fabricated using large ACS template.

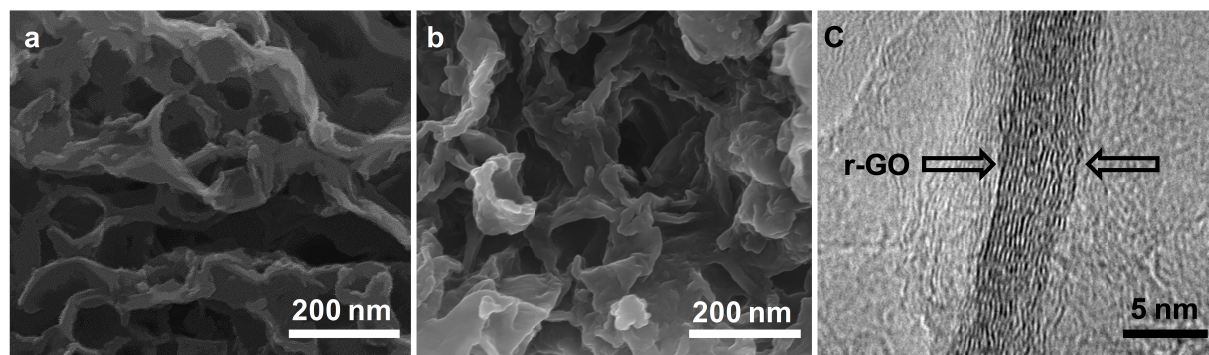


Figure S2. SEM images of a) HCS/RGO5 and b) HCS/RGO5-KOH, and c) TEM image of graphitic structure of r-GO sheet on HCS/RGO5-KOH.

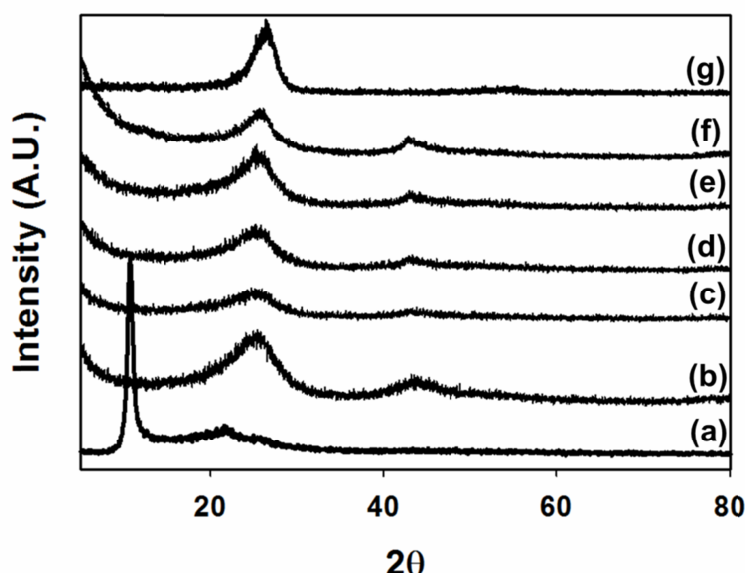


Figure S3. X-ray diffraction patterns of a) graphite oxide, b) CS, c) HCS/r-GO5, d) HCS/r-GO15, e) HCS/r-GO25, f) HCS/r-GO5-KOH, and g) r-GO.

The X-ray diffractograms (XRD) of graphite oxide, HCS, HCS/r-GO5, HCS/r-GO15, HCS/r-GO25, P-HCS/r-GO5, and r-GO indicate a crystallinity and structural transformation (Figure S3). After the oxidation of graphite, a prominent diffraction peak (002) at 26.5° (not shown here) was shifted to 10.7° due to the introduction of oxygen-containing functional groups and the intercalation of water molecules between layers as well (Figure S3a). However, thermal reduction of GO at 900° under Ar gas flow (with 2.7%) initiates the graphitization of sp^3 carbons, which causes the peak shift of (002) plane back to 26.3° (Figure S3f).⁴ As shown Figure S3b-e, the two broad peaks at 25.4° (002) and 44° (100) observed in CS demonstrate the generation of a weakly ordered graphitic carbon,⁵ and the (002) peak position of HCS/r-GO composites is located between that of CS and that of r-GO.

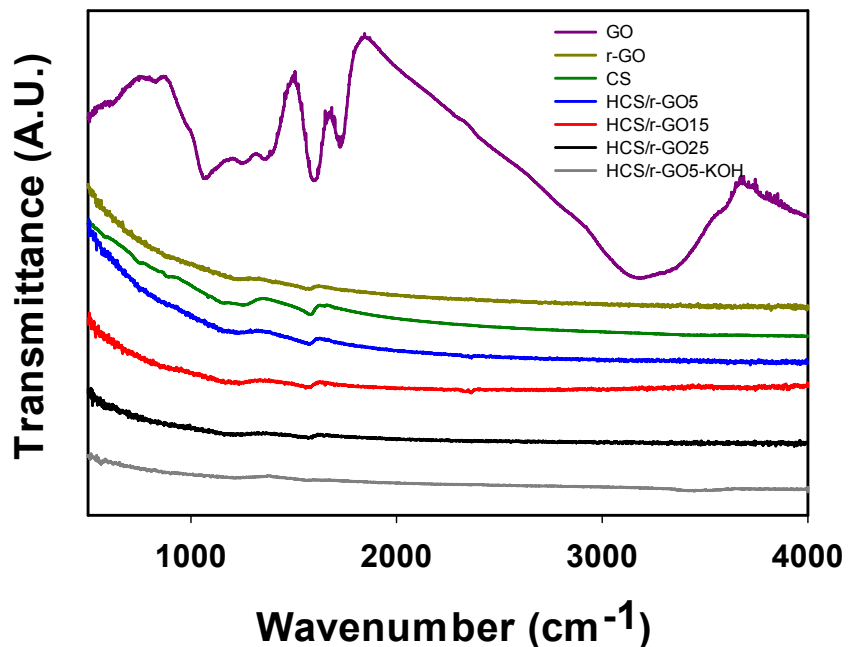


Figure S4. FT-IR spectra of GO, r-GO, CS, HCS/r-GO5, HCS/r-GO15, HCS/r-GO25, and HCS/r-GO-KOH.

The change of functional groups is monitored by FT-IR spectroscopy. Many vibration peaks such as O-H (3000-3400 cm^{-1}), C=O(1726 cm^{-1}), C=C (1602 cm^{-1}), C-O(1361 cm^{-1}), epoxy C-O(1252 cm^{-1}), and alkoxy C-O(1065 cm^{-1}) are observed in GO,⁶ whereas only two peak at 1579 cm^{-1} (C=C) and 1219 cm^{-1} (C-O) are seen in r-GO, CS, HCS/r-GO5, HCS/r-GO15, and HCS/r-GO25.⁷ This result means that thermal treatment at 900 °C under argon gas flow (with 2.7 % H₂) for 5hr is favorable for not only carbonization of a carbon source but also reduction of GO. The further chemical and thermal treatment (HCS/r-GO-KOH) showed minimal amount of surface functional groups.

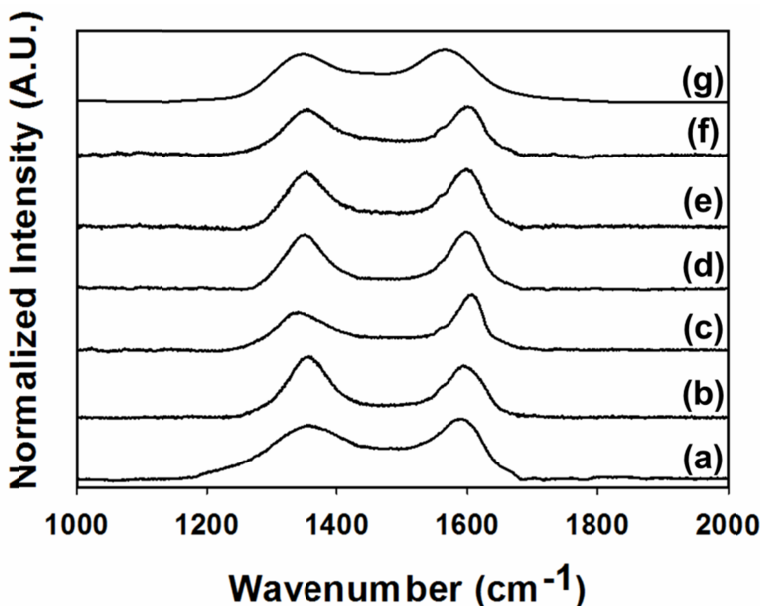


Figure S5. Raman spectra of a) GO, b) r-GO, c) CS, d) HCS/r-GO5, e) HCS/r-GO15, f) HCS/r-GO25, and g) HCS/r-GO5-KOH.

Raman spectroscopy associated with the electronic and structural properties of carbon networks exhibits D ($\sim 1355 \text{ cm}^{-1}$) and G ($\sim 1595 \text{ cm}^{-1}$) bands and their relative ratio. While the D band indicates a comparative measure of disorder and edge chirality, the G band represents a relative degree of graphitization.⁸ The G band of GO is located at 1589 cm^{-1} and its intensity is bigger than that of D band. After thermal reduction, the intensity of D band become bigger than that of G band and the G band shift is observed from 1589 to 1594 cm^{-1} as well. The chemical activation of the composite sample (Fig. S5g) caused D and G band shifts to lower wavenumbers again. In principle, the D/G intensity ratio should be reduced due to the recovery of sp^2 domains but the introduction of defects such as the splitting GO sheets into fragments causes the D/G intensity ratio increased, which is already observed by many research groups.⁹ The D/G intensity ratio of CS is much smaller than that of r-GO and the G band is observed at 1607 cm^{-1} . For the all composites, the D/G intensity ratio is measured about 1.⁴

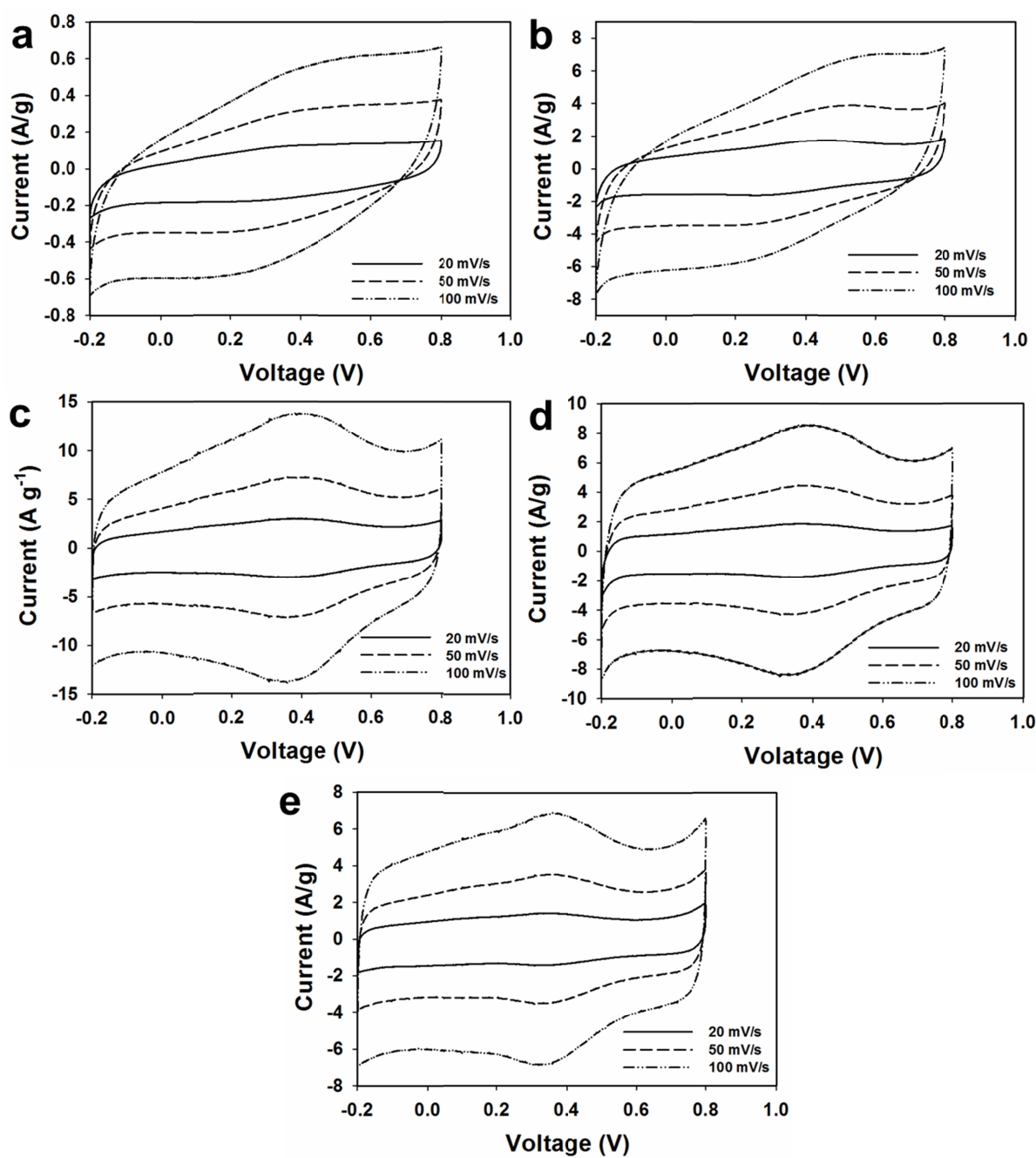


Figure S6. Cyclic voltammetry of a) r-GO, b) CS, c) HCS/r-GO5, d) HCS/r-GO15, and e) HCS/r-GO25 with increasing scan rates from 20 to 100 mV s⁻¹.

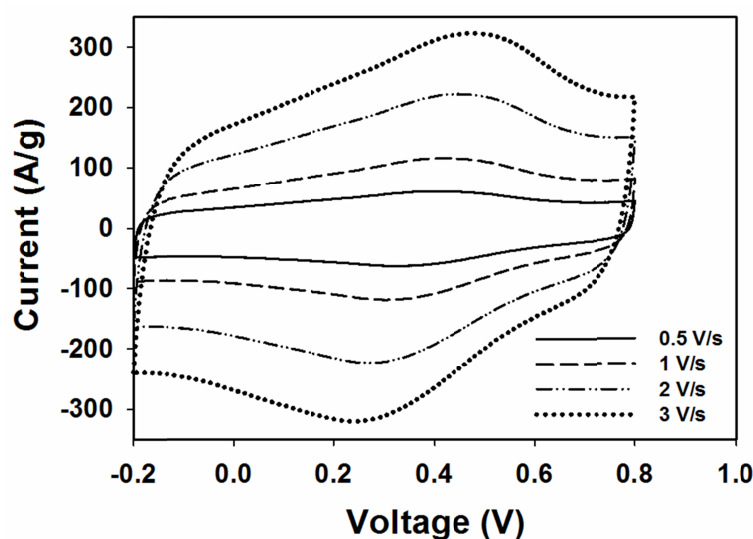


Figure S7. Cyclic voltammetry of HCS/r-GO5 at extremely high scan rates.

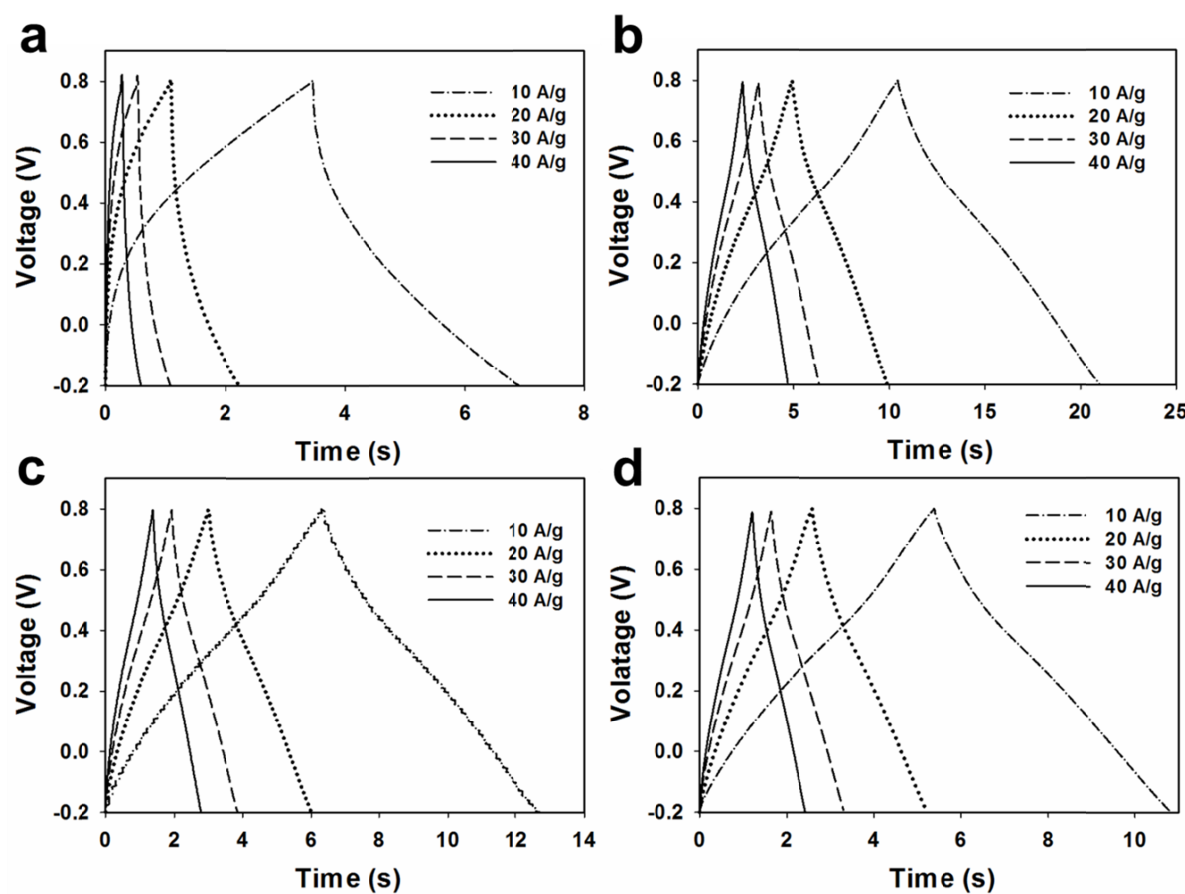


Figure S8. Galvanostatic charge-discharge curves of a) CS, b) HCS/r-GO5, c) HCS/r-GO15, and d) HCS/r-GO25 with increasing current density from 10 to 40 A g⁻¹.

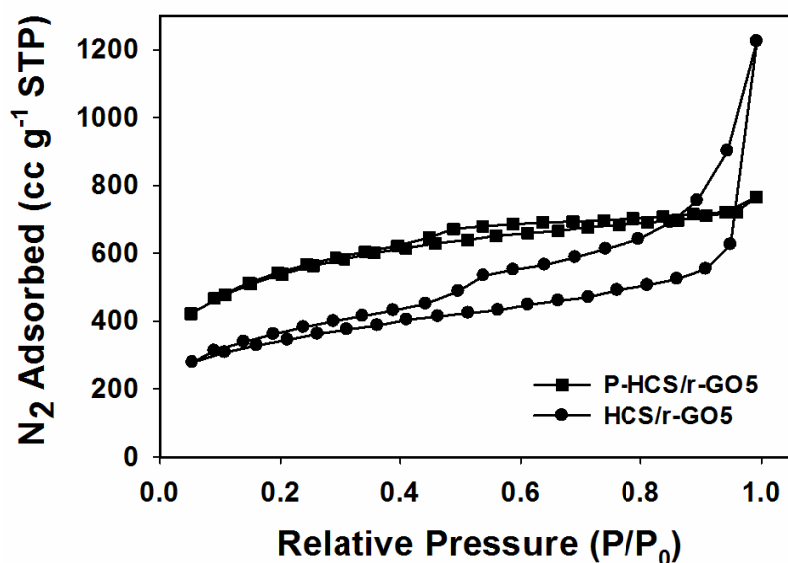


Figure S9. Nitrogen adsorption/desorption isotherms of before and after KOH activation of HCS/r-GO5.

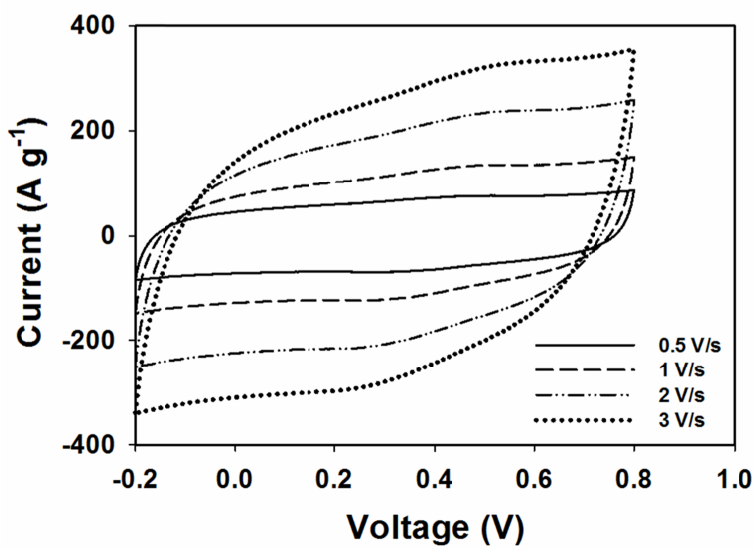


Figure S10. Cyclic voltammetry of HCS/r-GO5-KOH at extremely high scan rates.

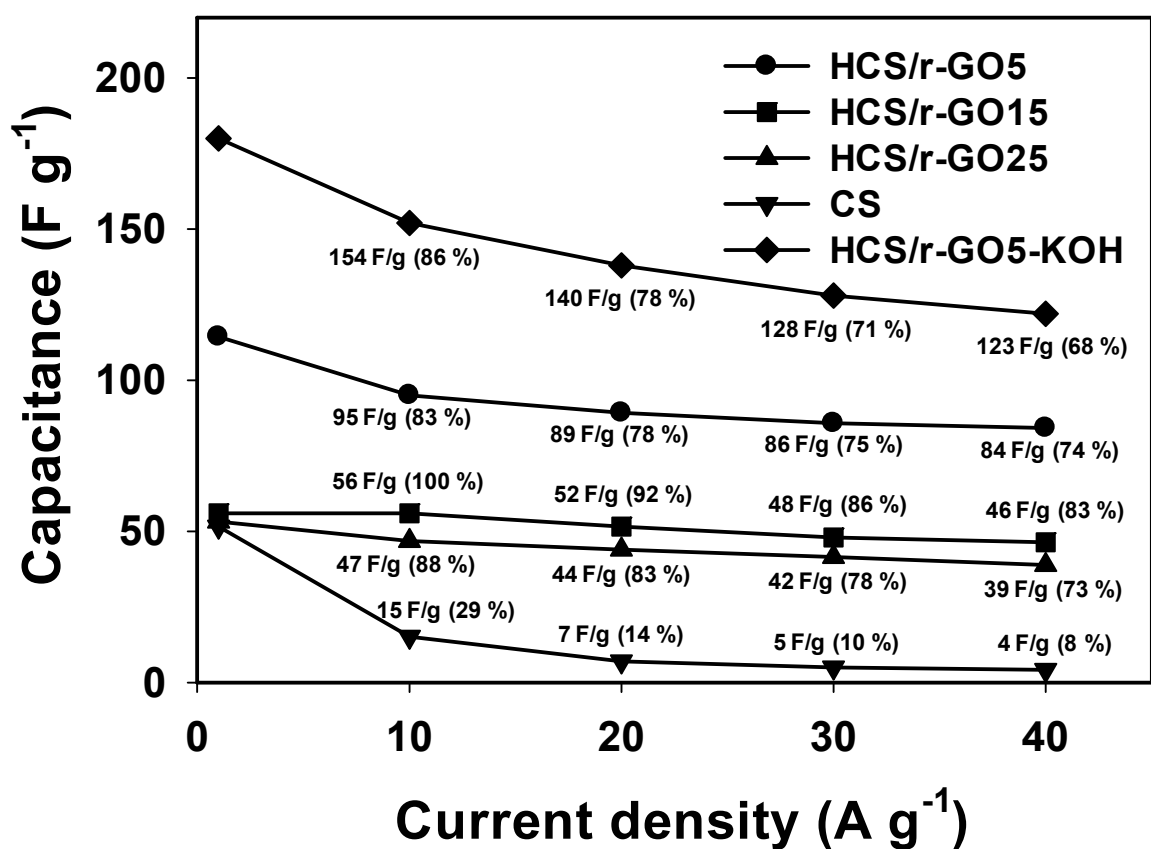


Figure S11. C_{sp} of CS, HCS/r-GO5, HCS/r-GO15, HCS/r-GO25, and HCS/r-GO5-KOH with increasing the current density. The C_{sp} of CS, HCS/r-GO5, HCS/r-GO15, HCS/r-GO25, HCS/r-GO5-KOH at a current density of 1 A g^{-1} shows 52, 114, 56, 53, and 180 F g^{-1} , respectively. Noted values are the C_{sp} and its retention at the specific current density.

Table S1. Properties of carbonaceous materials prepared using phenol and paraformaldehyde.

Samples	GO solution added (mL) ^[a]	GO/(phenol+PFA) ratio ^[b]	Surface area (m ² g ⁻¹)	Pore volume (cc g ⁻¹)	Pore size distribution (nm) ^[c]	Capacitance (F g ⁻¹) ^[d]
CS	0	-	492	0.211	3.7	52
r-GO	-	-	68	0.438	-	2
HCS/r-GO5	5	4.0	1175	1.176	4.2	114
HCS/r-GO15	15	11.0	450	0.312	4.2	56
HCS/r-GO25	25	17.0	290	0.144	3.7	53
HCS/r-GO5-KOH	5	4.0	1880	0.818	3.8	180

[a] GO solution of 2.5 mg mL⁻¹

[b] Synthesis ratios

[c] Maximum peak in the mesopore region (BJH method based on the desorption branch)

[d] At a current density of 1.0 A g⁻¹.

References

- (1) Kovtyukhova, N. I.; Ollivier, P. J.; Martin, B. R.; Mallouk, T. E.; Chizhik, S. A.; Buzaneva, E. V.; Gorchinskiy, A. D. *Chem. Mater.* **1999**, *11*, 771-778.
- (2) Yoon, S. B.; Sohn, K.; Kim, J. Y.; Shin, C. H.; Yu, J. S.; Hyeon, T. *Adv. Mater.* **2002**, *14*, 19-21.
- (3) Gamby, J.; Taberna, P.L.; Simon, P.; Fauvarque, J.F.; Chesneau, M. *J. Power Source* **2001**, *101*, 109-116.
- (4) Gao, W.; Alemany, L. B.; Ci, L.; Ajayan, P. M. *Nat. Chem.* **2009**, *1*, 403-408.
- (5) Liu, J.; Shao, M.; Tang, Q.; Chen, X.; Liu, Z.; Qian, Y. *Carbon* **2002**, *41*, 1645-1648.
- (6) Xu, Y.; Bai, H.; Lu, G.; Li, C.; Shi, G. *J. Am. Chem. Soc.* **2008**, *130*, 5856-5857.
- (7) Park, S.; An, J.; Jung, I.; Piner, R. D.; An, S. J.; Li, X.; Velamakanni, A.; Ruoff, R. S. *Nano Lett.* **2009**, *9*, 1593-1597.
- (8) Eda, G.; Chhowalla, M. *Adv. Mater.* **2010**, *22*, 2392-2415.
- (9) Stankovich, S.; Dikina, D. A.; Pinera, R. D.; Kohlhaasa, K. A.; Kleinhammesc, A.; Jia, Y.; Wu, Y.; Nguyen, S. T.; Ruoff, R. S. *Carbon* **2007**, *45*, 1558-1565.